PHYSICAL REVIEW B **82**, 081406(R) (2010)

Aligning electronic energy levels at the TiO_2/H_2O interface

Jun Cheng and Michiel Sprik*
Department of Chemistry, University of Cambridge, Cambridge CB2 1EW, United Kingdom
(Received 22 July 2010; published 12 August 2010)

The electronic energy levels of a model titanium dioxide water interface computed using the Perdew-Burke-Ernzerhof (PBE) density functional are positioned relative to the normal hydrogen electrode and vacuum. As energy reference we use the solvation free energy of the H^+ ion computed by reversible insertion of a proton in the aqueous part of the model system. The interaction with water raises the energy levels bringing the conduction-band edge in fair alignment with experiment. The error in the PBE band gap must therefore be largely attributed to underestimation of the ionization potential.

DOI: 10.1103/PhysRevB.82.081406 PACS number(s): 73.20.−r, 71.15.Pd, 82.65.+r

The photoelectrochemical activity of a semiconductor-liquid interface crucially depends on the relative positions of the electronic energy levels at the two sides of the interface.[1–3] The conventional reference for redox free energies of aqueous solutes is the normal hydrogen electrode (NHE). The key question is therefore, where to place the band structure of the solid electrode relative to the NHE. Considering the success of the application of density-functional theory (DFT) based electronic-structure calculation in surface science,[4] it would seem that the same methods could be of use for solid-liquid interfaces. A precondition for the extension to aqueous electrochemistry is conversion of the calculated electronic energies to the NHE scale.[5–7] In earlier publications we have developed a DFT-based molecular-dynamics (DFTMD) implementation of such a computational hydrogen electrode.[8,9] In the present contribution this scheme is applied in a computation of the flat-band potential of the rutile $TiO_2(110)/H_2O$ interface at the point of zero net proton charge (PZC).[1,2] This result is used to analyze the contribution of adsorbed water molecules to the interface potential at the PZC.

The electrical double layer formed at a TiO_2-water interface has both an electronic and ionic component. The interfacial potential established by exchange of electrons with the redox-active electrolyte can be eliminated by the application of an appropriate bias, the flat-band potential (FBP), which can be determined from capacitance measurements.[10] Since the conduction-band edge (CBE) of TiO_2 electrodes practically coincides with the Fermi level within 0.1 eV difference,[3] the FBP is generally regarded as an estimate of the CBE free of space-charge effects. The origin of the ionic contribution to the surface potential is proton exchange with the electrolyte. The proton surface charge is compensated by ions in solution. The surface potential controlled by this process can be minimized by measuring the FBP under PZC conditions. The corresponding CBE will be indicated by CBE_0. For TiO_2 rutile (110) with a PZC of about 5 the $CBE_0=-0.35$ V versus NHE.[10] This can be represented as an absolute energy level with respect to vacuum by adding 4.44 V for the absolute NHE potential.[11] The result is a CBE_0 of −4.10 eV.[2] The band gap ΔE_g is relatively insensitive to applied voltage or pH. Reference 2 uses the value of $\Delta E_g=3.0$ eV placing the valence-band edge (VBE) at $VBE_0=-7.10$ eV.

Reduction of TiO_2 by the NHE is a multiphase reaction involving addition of an electron to the solid (s) coupled to transfer of an H^+ ion from the gas phase (g) to the aqueous electrolyte (aq).

$$TiO_2(s) + e^-(vac) + H^+(g) \rightarrow TiO_2^-(s) + H^+(aq), \qquad (1)$$

where $e^-(vac)$ is an electron at rest in vacuum. Adding the formation free energy $\Delta_f G_{H^+(g)}$ of the gas-phase proton $[1/2H_2(g) \rightarrow e^-(vac) + H^+(g)]$ to the free energy of reaction 1 gives the negative of the electron affinity (EA) of aqueous TiO_2 versus NHE. Alternatively we can subtract the absolute solvation free energy $\Delta_s G_{H^+}$ of the proton and obtain the value of −EA with respect to vacuum. For $\Delta_f G_{H^+(g)}$ we use the experimental value of 15.81 eV quoted in Ref. 11. $\Delta_s G_{H^+}$ is set equal to the estimate of −11.53 eV obtained in Ref. 12 from mass spectrometry [for convenience gas-phase standard states have been converted from 1 bar to 1 mol dm^{-3} (Refs. 9 and 12)]. Note that there is a 160 meV mismatch between $-\Delta_s G_{H^+} - \Delta_f G_{H^+(g)} = -4.28$ eV and the −4.44 eV energy level of the NHE of Ref. 11. This difference is consistent with the surface potential of water[13] suggesting that this is missing from the $\Delta_s G_{H^+}$ of Ref. 12. Here we use the uncorrected value.

The design of the computational NHE of Ref. 9 was motivated by the DFTMD simulation of proton-coupled redox reactions which requires an unified treatment of reduction and protonation. Solvation of a proton $[H^+(g) \rightarrow H^+(aq)]$ is replaced by the protonation of a water molecule $[H^+(g) + H_2O(l) \rightarrow H_3O^+(aq)]$. This changes reaction 1 into

$$TiO_2(s) + e^-(vac) + H^+(g) + H_2O(l) \rightarrow TiO_2^-(s) + H_3O^+(aq). \qquad (2)$$

This modification allows us to employ the reversible deprotonation method of Ref. 14. This scheme was developed for the DFTMD computation of pK_a in the framework of the Brønsted picture of acidity (see also Ref. 9). Rather than eliminating the proton completely, the nuclear charge is switched off changing the proton into a dummy. Applied to the hydronium ion this fictitious chemical transformation can be written as $H_3O^+ \rightarrow H_2Od$ with d representing the dummy. Particle d is held in place by a harmonic potential binding it to the H_2O molecule in a geometry approximately similar to that of a proton in a hydronium ion avoiding the highly unstable configurations that might otherwise arise when the

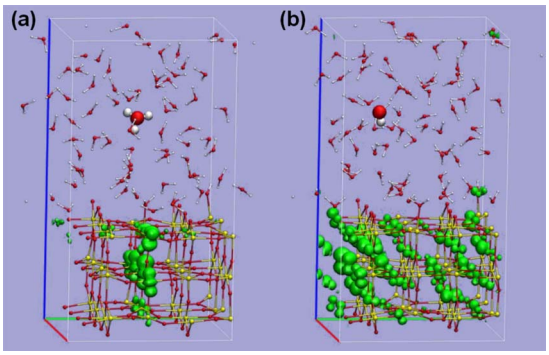

FIG. 1. (Color online) Model TiO_2/H_2O interface with (a) an excess electron in the solid slab and proton in the water layer in between slabs and (b) a hole and a compensating OH^- in solution. Red (dark gray) balls are O, white balls H, and small yellow (light gray) balls Ti. H_2O molecules with added or removed H are highlighted. The spin density is visualized by isosurfaces in green (gray) (density is 1.5×10^{-3}).

charge is switched back on. Equally important, the directed protonation enables us to select the H_2O molecule providing the NHE energy reference. This molecule must be located away from the surface in the water compartment of the DFTMD model system, where bulk liquid conditions are assumed to apply (see Fig. 1).

The anodic electron in reaction 2 is easier to implement. All we have to do is adjusting the number of electrons in the self-consistent-field cycle. The electron count is incremented at the same time as the charge of the dummy proton is restored. This operation is carried out for a set of fixed atomic configurations sampled from a long DFTMD trajectory. The result is a series of vertical energy gaps ΔE. The reaction free energy is obtained from these data by thermodynamic integration.[9] The key auxiliary quantity in this approach is a mapping potential $E_\eta=(1-\eta)E_0+\eta E_1$, where η is a coupling parameter and E_0 and E_1 are the potential-energy surfaces of the reactant, respectively, product state. The derivative of E_η with respect to η is the vertical energy gap $\Delta E=E_1-E_0$. The thermal average $\langle\Delta E\rangle_\eta$ in the ensemble defined by E_η integrated over the coupling parameter gives the reaction free energy. The thermodynamic integral for reaction 1 is the basic input for the calculation of the EA of the TiO_2/H_2O interface. Similarly the ionization potential (IP) is estimated from the free energy cost of oxidizing the solid in conjunction with transfer of a proton from a reference water molecule to the gas phase.

$$TiO_2(s) + H_2O(l) \rightarrow TiO_2^+(s) + OH^-(aq) + e^-(vac) + H^+(g). \tag{3}$$

Reaction 3 uses the absolute deprotonation free energy of a water molecule as a reference. This quantity, indicated by $\Delta_{dp}G_{H_2O}$, differs from the absolute solvation free energy of the proton by $-k_BT\ln K_d=1.03$ eV, where K_d is the ionic dissociation constant of water. This gives $\Delta_{dp}G_{H_2O}=-\Delta_sG_{H^+}-k_BT\ln K_d=12.56$ eV.

To compute the CBE_0 the aqueous electrode is modeled by a piece of defect-free TiO_2 in contact with pure water (see Fig. 1). This raises a number of questions. There is first of all the problem of the bias V_0 in the electrostatic potential introduced by the application of periodic boundary conditions (PBCs). V_0 has no physical meaning and cannot be determined without an explicit interface with vacuum (see, e.g., Ref. 7). For determination of EA or IP versus NHE this is not an issue because the charges of the condensed phase products in reactions 2 and 3 add up to zero. Electrode potentials are, however, adiabatic electronic energies. The vertical IP and EA and the Kohn-Sham (KS) energy levels are of interest as well. Rather than inserting vacuum layers in the model system to provide a reference for absolute values for vertical energies,[5–7] we follow the approach of Ref. 8 and align the solvation free energy of the proton computed under PBC with experiment.

A further point of concern is the bias introduced by the restraining potentials. This question was analyzed in some detail in Ref. 9. Modeling the deprotonation of a hydronium ion $H_3O^+(aq)\rightarrow H_2O(l)+H^+(g)$ by the dummy atom transformation $H_3O^+(aq)\rightarrow H_2Od(aq)$ changes the entropy balance. In addition we must correct for zero-point motion which is not accounted for in DFTMD simulation which treats protons as classical particles. The thermochemical correction we derived in Ref. 9 capturing these effects can be written as

$$\Delta A_c = -k_BT\ln\left(\rho_{H_2O}\Lambda_{H^+}^3\frac{q_{H_2Od}}{q_{H_2O}}\right)+\Delta E_{ZPM}, \tag{4}$$

where $\rho_{H_2O}=55.5$ mol dm^{-3} is the ambient density of liquid water and Λ_{H^+} the thermal wavelength of the proton. The product $\rho_{H_2O}\Lambda_{H^+}^3$ accounts for the liberation entropy of the proton. q_{H_2Od} and q_{H_2O} are the gas-phase vibrational and rotational partition functions of a water molecule with dummy attached (H_2Od) and without (H_2O). The ratio q_{H_2Od}/q_{H_2O} corrects for the entropy introduced by the three extra degrees of freedom of the dummy. Finally, ΔE_{ZPM} is a correction for the zero-point motion of the H_3O^+ in solution. The thermochemical correction ΔA_c of Eq. (4) is uncomfortably large. The estimate we give in Ref. 9 is $\Delta A_c=0.5$ eV (see also Ref. 15). This 0.5 eV must be added to the DFTMD solvation free energy of the proton and therefore included in the free-energy change in the NHE reactions 2 and 3.

All simulations have been carried out using the freely available CP2K/QUICKSTEP package.[16] The orbitals are represented in a Gaussian-type double-ζ basis with one set of polarization function (DZVP). The electron density is reexpanded in a plane-wave auxiliary basis with a 280 Ry cutoff. Core electrons are taken into account by analytic Goedecker-Teter-Hutter pseudopotentials. The DFT was implemented at the generalized gradient approximation Perdew-Burke-Ernzerhof (GGA-PBE) level. The convergence criterion for electronic optimization is set to 3×10^{-7} a.u. for the electronic gradient and 10^{-13} a.u. for the total energy. The time step for the Born-Oppenheimer propagation scheme was 0.5 fs. The temperature was controlled by a Nosé-Hoover thermostat with the target temperature of 330 K. The lengths of MD trajectories are between 5 and 10 ps. The rutile $TiO_2(110)$ surface has been modeled by a periodic slab of three O-Ti-O trilayers with a 4×2 surface

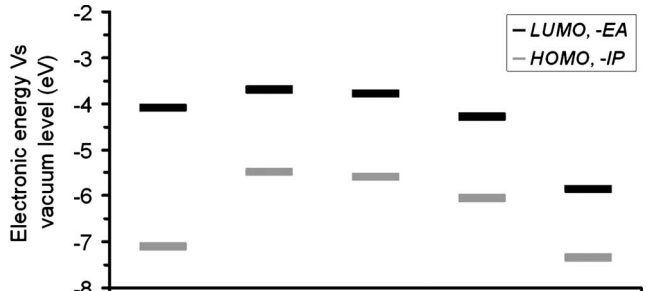

	Exp.	Adiabatic TiO2/H2O	Vertical TiO2/H2O	TiO2_1ML H2O/Vac.	TiO2/Vac.
LUMO, -EA	-4.1	-3.7	-3.8	-4.3	-5.9
HOMO, -IP	-7.1	-5.5	-5.6	-6.1	-7.4

FIG. 2. Computed conduction- and valence-band edges of the TiO_2/H_2O interface compared to the experiment (Ref. 2), the clean surface in vacuum and a surface with 1 ML of H_2O.

cell. Periodic images of the slab are separated by 15 Å leading to a supercell of $11.9\times13.2\times24.2$ Å^3. The space between TiO_2 slabs is fully filled in with 71 water molecules creating two symmetric interfacial planes in the MD cell. A very similar methodology was used in the calculation of the PZC of TiO_2/H_2O in Ref. 15, where a more detailed description can be found. Spin polarization is used whenever necessary.

The main result of the calculation consists of estimates of the adiabatic and vertical EA and IP of the TiO_2/H_2O model system corresponding to two different values for the CBE and VBE. Energies calculated under PBC will be marked by a bar. Using a three-point approximation to the thermodynamic integrals the free-energy change of the (reverse) reduction reaction 2 is estimated as $\bar{E}A=15.7$ eV. For the free-energy change of the oxidation reaction 3 we obtained $\bar{I}P=18.6$ eV. With mentioned corrections this gives an adiabatic CBE at $-\bar{E}A+\Delta_f G_{H^+(g)}+\Delta A_c=0.6$ eV above the NHE level or an electrode potential of −0.6 V. This must be compared to −0.35 V for the experimental CBE_0. The computed oxidation free energy leads to an adiabatic VBE at $-\bar{I}P+\Delta_f G_{H^+(g)}-k_BT\ln K_d+\Delta A_c=-1.2$ below the NHE level, which is equivalent to an electrode potential of +1.2 V compared to +2.65 V in experiment. Alternatively the levels can be represented on an absolute scale relative to vacuum. For the CBE this gives $-EA=-\bar{E}A-\Delta_s G_{H^+}+\Delta A_c=-3.7$ eV and $-IP=-\bar{I}P+\Delta_{dp}G_{H_2O}+\Delta A_c=-5.5$ eV for the VBE. These results are summarized in the Fig. 2 together with the experimental values.

The vertical band edges are computed as the highest occupied molecular orbital (HOMO) and the lowest unoccupied molecular orbital (LUMO). This is common practice in band-structure calculation and is justified by the extended nature of the one-electron states in solids.[17] For the DFTMD averaged HOMO of the periodic supercell we find $\bar{\epsilon}_{HOMO}=1.3$ eV with the LUMO at $\bar{\epsilon}_{LUMO}=3.1$ eV. Evidently the orbital energies are shifted by the PBC to positive energies. The V_0 correcting this shift is estimated by comparing the solvation free energy of the proton evaluated for the same cell to the experimental value. The solvation free energy we computed using the reversible proton insertion method is $\Delta_s\bar{G}_{H^+}=-18.9$ eV, yielding $qV_0=\Delta_s G_{H^+}-\Delta_s\bar{G}_{H^+}-\Delta A_c=6.9$ eV (q is the unit charge). The absolute positions of the vertical CBE and VBE are therefore $\epsilon_{LUMO}=\bar{\epsilon}_{LUMO}-qV_0=-3.8$ eV and $\epsilon_{HOMO}=\bar{\epsilon}_{HOMO}-qV_0=-5.6$ eV.

The computed vertical and adiabatic CBE and VBE are compared in Fig. 2. The statistical uncertainty for these energies is about 0.2 eV. In view of this error margin, the agreement between vertical and adiabatic levels is remarkable. This suggests that solvation has little effect on the excess electron and hole in our model system. Delocalization minimizes the interaction with polar solvent molecules. Examining the spin densities of excess electron and hole, as illustrated in Fig. 1, we see that, indeed, both states are delocalized but the extent of delocalization is different: the hole [Fig. 1(b)] is fully distributed over all the O atoms in the TiO_2 slab while the excess electron [Fig. 1(a)] is shared by Ti atoms restricted to a plane vertical to the 110 surface with a tendency to accumulate in the subsurface layer. The coupling between the lattice and the semilocalized excess electron is too weak to induce a gap state. This result must be considered with caution in view of the tendency of GGA-type density functionals, such as PBE, to overstabilize delocalized states.[17,18] The advantage is that the adiabatic EA computed by PBE/DFTMD can indeed be regarded as representing the conduction-band edge.

The CBE we calculate is about 0.4 eV above the CBE_0 of experiment. From the perspective of photoelectrochemistry this is a significant discrepancy. However, considering the various sources of error in the calculation, we are inclined to consider this as encouraging agreement. The result for the IP (1.6 eV too small) is considerably worse. This suggests that the explanation for the 1.2 eV underestimation of the band gap (1.8 versus 3.0 eV) must be sought in the GGA treatment of the holes in the valence band rather than that of electrons in the conduction band. To investigate the effect of hydration on EA and IP we have computed the orbital energies of a clean slab of TiO_2 of the same size in vacuum and a slab covered on both sides with a monolayer (ML) of H_2O. KS levels were put on an absolute scale using conventional surface science methods. We find the LUMO of the clean slab positioned at $\epsilon_{LUMO}=-5.9$ eV with a gap of $\Delta E_g=1.5$ eV (changing to $\epsilon_{LUMO}=-5.5$ eV and $\Delta E_g=1.8$ eV for the five-layer slab). For the 1 ML system the results are $\epsilon_{LUMO}=-4.3$ eV with a gap of $\Delta E_g=1.8$ eV (changing to $\epsilon_{LUMO}=-4.0$ eV and $\Delta E_g=1.9$ eV for the five-layer system). DFT places the CBE of a vacuum slab 2.1 eV below the CBE of the aqueous interface. However, a single monolayer moves the CBE up by 1.6 eV leaving a 0.5 gap with the CBE in full solution.

Finite system size effects are a major concern in application of electronic-structure calculation to interfacial electrochemistry. For example, it has been pointed out by Rossmeisl *et al.*[7] that addition of only a single electron and compensating counterion represents a significant change in the surface charge density leading to an increase in the total energy due to capacitive charging. This effect would directly perturb the adiabatic EA in our calculation. The agreement between the adiabatic EA and the LUMO of the uncharged system can

therefore be seen as reassurance that our system is large enough to avoid these difficulties. A further conspicuous finite system size effect is the odd-even oscillation of the band gap with the thickness of a clean TiO_2 slab in vacuum.[19] The costs of DFTMD calculations prohibit a detailed analysis of system-size dependence in solution. However, as already mentioned, covering a vacuum slab on both sides with 1 ML of H_2O molecules, saturating the coordination of the Ti_{5c} sites, had the effect of suppressing these oscillations well below the 100 meV threshold.

In summary the computational NHE we have developed uses the solvation free energy of H^+ as energy reference in close analogy with the real electrochemical NHE. Applying this scheme we computed the position of the conduction-band edge of a model aqueous TiO_2 electrode which was found 0.4 eV above the experimental level. Considering the limitations in the accuracy of GGA functionals for the calculation of band gaps, this result is better than expected. Our result for the CBE can be therefore be considered as support for the DFT studies of electron injection in dye-sensitized solar cells that have appeared in the literature (see, for example, Ref. 20). The downside of the encouraging result for the electron affinity is the serious underestimation of the ionization potential profoundly frustrating attempts at GGA level studies of photo-oxidation by TiO_2 electrodes. We also showed that the contribution of hydration to the TiO_2 interface potential is comparable or even larger than the shift in the position of the energy levels due to variation in the pH. We regard this application to TiO_2/H_2O as a proof of principle of our DFTMD scheme as well as an illustration of the importance of the introduction of an absolute energy reference in interface calculations.

Marialore Sulpizi and Joost VandeVondele are acknowledged for their contribution to the development of method and code. J.C. is grateful to EPSRC for financial support. The calculations have been performed using resources provided by the UKCP consortium.

*ms284@cam.ac.uk

[1] A. Fujishima, X. Zhang, and D. A. Tryk, Surf. Sci. Rep. **63**, 515 (2008).
[2] M. Grätzel, Nature (London) **414**, 338 (2001).
[3] N. Sato, *Electrochemistry at Metal and Semiconductor Electrodes* (Elsevier Science & Technology, Oxford, 1998).
[4] *Chemical Bonding at Surfaces and Interfaces*, edited by A. Nilsson, L. G. M. Petterson, and J. K. Nørskov (Elsevier, Amsterdam, 2008).
[5] C. D. Taylor, S. A. Wasileski, J.-S. Filhol, and M. Neurock, Phys. Rev. B **73**, 165402 (2006).
[6] O. Sugino, I. Hamada, M. Otani, Y. Morikawa, T. Ikeshoji, and Y. Okamoto, Surf. Sci. **601**, 5237 (2007).
[7] J. Rossmeisl, E. Skúlason, M. E. Björketun, V. Tripkovic, and J. E. Nørskov, Chem. Phys. Lett. **466**, 68 (2008).
[8] C. Adriaanse, M. Sulpizi, J. VandeVondele, and M. Sprik, J. Am. Chem. Soc. **131**, 6046 (2009).
[9] J. Cheng, M. Sulpizi, and M. Sprik, J. Chem. Phys. **131**, 154504 (2009).
[10] L. Kavan, M. Grätzel, S. E. Gilbert, C. Klemenz, and H. J. Scheel, J. Am. Chem. Soc. **118**, 6716 (1996).
[11] S. Trasatti, Pure Appl. Chem. **58**, 955 (1986).
[12] M. H. Tissandier, K. A. Cowen, W. Y. Feng, E. Gundlach, M. H. Cohen, A. D. Earhart, and J. V. Coe, J. Phys. Chem. A **102**, 7787 (1998).
[13] W. R. Fawcett, Langmuir **24**, 9868 (2008).
[14] M. Sulpizi and M. Sprik, Phys. Chem. Chem. Phys. **10**, 5238 (2008).
[15] J. Cheng and M. Sprik, J. Chem. Theory Comput. **6**, 880 (2010).
[16] The CP2K developers group, 2008, http://cp2k.berlios.de
[17] P. Mori-Sánchez, A. J. Cohen, and W. Yang, Phys. Rev. Lett. **100**, 146401 (2008).
[18] C. Di Valentin, G. Pacchioni, and A. Selloni, Phys. Rev. Lett. **97**, 166803 (2006).
[19] T. Bredow, L. Giordano, F. Cinquini, and G. Pacchioni, Phys. Rev. B **70**, 035419 (2004).
[20] W. R. Duncan and O. V. Prezhdo, Annu. Rev. Phys. Chem. **58**, 143 (2007).